

Granulometric and Petrographic Assessment of the Textural, Mineralogical and Paleoenvironment of Deposition of Gulma Sandstone Member, Gwandu Formation, Sokoto Basin, Northwestern Nigeria

Ola-Buraimo A. Olatunji. and Musa Rukaya

Received: 24 February 2024/Accepted: 21 May 2024/Published: 10 June 2024

Abstract: Granulometric analysis was carried out on sandstone samples collected from the Gulma Area, a suburb of Argungu town, Kebbi State, Nigeria. The sandstone facies were investigated to determine textural characteristics, transportation history, maturity, and paleoenvironment of deposition of the sediments. Heavy mineral analysis and mineral point count were carried out to determine the sandstone's mineralogical and textural maturity. The standard sieve analysis method was employed by arranging sieves in order of size with the coarsest at the top and the finest size at the bottom with a basal attached pan. The sieve shaker was allowed to operate for fifteen minutes to allow separation of various grain sizes. Field observation revealed that the lithostratigraphic section is composed of nine repetitive layers. The main lithofacies are purplish, moderately bioturbated, liesegang ring structure sandstone, yellowish nodular claystone, and continental massive reddish claystone. The topmost beds are continental massive reddish mudstone and ferruginized granules stone as the capping facies which is different from the commonly oolitic ironstone that characterized the top of the Gwandu Formation. A characteristic liesegang ring structure is present in the Gulma Sandstone Member which is a unique appearance in Gwandu Formation. Cumulative frequencies were plotted whereby textural statistical parameters such as mean, standard deviation (sorting), skewness and kurtosis were calculated. The mean values of the samples vary from 2.2-2.26 with an average of 1.86, indicative of fine sand class. The sorting values range between 1.2-1.216 with an average value of 1.196, indicative of poorly sorted particles,

characterized by tidal current deposits of high energy. The skewness values vary between -0.447 to -0.1 (ave. 0.198), which is negatively skewed. Kurtosis values range from 0.7-1.82, classified into very leptokurtic, platykurtic and leptokurtic classes. The paleoenvironment of deposition was deduced using multivariate values which range from -9.07 to -5.90; suggestive of marginal marine setting of a tidal and tidal shelf deposition. The Gulma Sandstone Member of the Gwandu Formation is a texturally and mineralogically submatured sediment.

Keywords: Granulometric, Liesegang, Tidal, Texturally and Mineralogically sub-matured

Ola-Buraimo A. Olatunji

Department of Geology, Federal University Birnin Kebbi, Kebbi State, Nigeria

Email: rolaburaimo@yahoo.com

Orcid id: 0000-0001-9601-1545

Musa Rukaya

Department of Geology, Federal University Birnin Kebbi, Kebbi State, Nigeria

Email: rukayyamusa267@gmail.com

1.0 Introduction

The Granulometric study of the Gwandu Formation has not been fully explored, and the information on the formation looks exhaustive. A further field study on the Gwandu Formation in another frontier out of Gwandu Emirate to other places like Argungu Emirate brings out new information on the sedimentation processes and paleoenvironment of deposition of the Gwandu Formation. Sieve analysis was used in deciphering the processes of transportation, deposition and maturity

indices of the Gwandu Sandstones of which much work has not been documented on it. The only recorded earlier research work on the sedimentology of Sokoto Basin was that of Ozumba *et al.* (2017). One of the few recent works is those of Ola-Buraimo *et al.* (2018); Ola-Buraimo and Usman (2022) which dwelled on the geochemistry and mineralogical maturity of Dukku Sandstone Member; Ola-Buraimo *et al.* (2022) on the sandstone textural properties and paleoenvironment of deposition of the Dukku Sandstone Type Locality of Gwandu Formation. Followed by the textural and depositional paradigm of Middle Neritic environmental system of the Kola Siltstone Type Section of Gwandu Formation (Ola-Buraimo *et al.*, 2022) and the geochemistry and petrographic study of the Jodu Sandstone in Gwandu Formation (Ola-Buraimo *et al.*, 2023). All these studies are concentrated in the Gwandu Emirate without any reports in Argungun Area, known for good outcrops of the Gwandu Formation.

The geologic evolution of the Sokoto Basin is similar to other sedimentary basins in Nigeria; formed as a result of rifting, but followed by the incursion of Mediterranean and Gulf of Guinea seas from the north and southern Nigeria respectively (Ola-Buraimo *et al.*, 2022). Some of the earlier workers in the Sokoto Basin include Falconer (1911), Kogbe (1981, 1989), Obiosio *et al.* (1991), Obaje (2009), Obaje *et al.* (2013), and Hamidu *et al.* (2024). Four sedimentary depositional phases were advanced to have been responsible for the deposition of rocks in Sokoto Basin; though this assertion is doubtful and most unlikely. It was described to be in multifaceted depositional phases (Ola-Buraimo and Mohammed, 2024).

The first phase referred to as pre-Maastrichtian in age led to the deposition of Gundumi and Illo Formations which are gritty and poorly sorted, deposited on Basement Crystalline rocks (Kogbe, 1979, 1981). The second phase is characterized by Maastrichtian age deposits known as Rima Group, consisting of Taloka, Wuro Formations, and separated unconformably by

the fossiliferous, calcareous and shaley Dukamaje Formation. The younger Paleocene age sediments are contained in the Sokoto Group, made up of Dange, Klambaina, and Gamba Formations. The Paleocene age ascribed to this group has been debunked, whereby, the Kalambaina Formation was dated as Early Maastrichtian to Paleocene (Ola-Buraimo and Meshack, 2024) and the Gamba Formation was dated as Middle Eocene based on palynomorph marker recoveries (Ola-Buraimo and Mohammed, 2024).

Therefore, the term Sokoto Group has been proven not to be an acceptable nomenclature for the Wurno, Kalambaina, and Gamba Formations (Ola-Buraimo and Mohammed, 2024; Ola-Buraimo and Meshack, 2024). An unconformable marine sandstone facies separates the older underlying Kalambaina Formation from the younger overlying Gamba Formation (Ola-Buraimo and Mohammed, 2024). The fossiliferous limestone beds of the Kalambaina Formation belong to the 1st and 2nd cycles of flooding surfaces, characterized by *Roselina koeneni* bio-events, of a Transgressive System Tract (Ola-Buraimo and Meshack, 2024).

The fourth phase of the sediment evolution in Sokoto Basin led to the deposition of Gwandu Formation, characterized by lithofacies ambiguity, the presence of mega fossils, different structures such as cross-bedding, bedding, lamination, joint, fracture, fault, channels, truncations, clinoforn structure, loadcast, bioturbation, ichnofossils, unconformity, and herringbone structures; deposited in varied environments from continental though marginal marine to typical marine setting, dated Early Miocene based on the recovery of pollen marker fossils (Ola-Buraimo *et al.*, 2018; Ola-Buraimo and Haidara, 2022; Ola-Buraimo and Usman, 2022; Ola-Buraimo *et al.*, 2022 a and b; Ola-Buraimo *et al.*, 2023a and b).

Therefore, the present study was based on further investigation of the lithosequence of Gwandu Formation, sedimentation processes, textural properties, maturity and paleoenvironment of deposition. The study



area is located within Gulma Town, in Argungu Local Government Area, Kebbi State, Nigeria. The area lies between

Latitude $N12^{\circ} 39' 20''$ to Longitude $E4^{\circ} 2' 13''$. (Fig. 1).

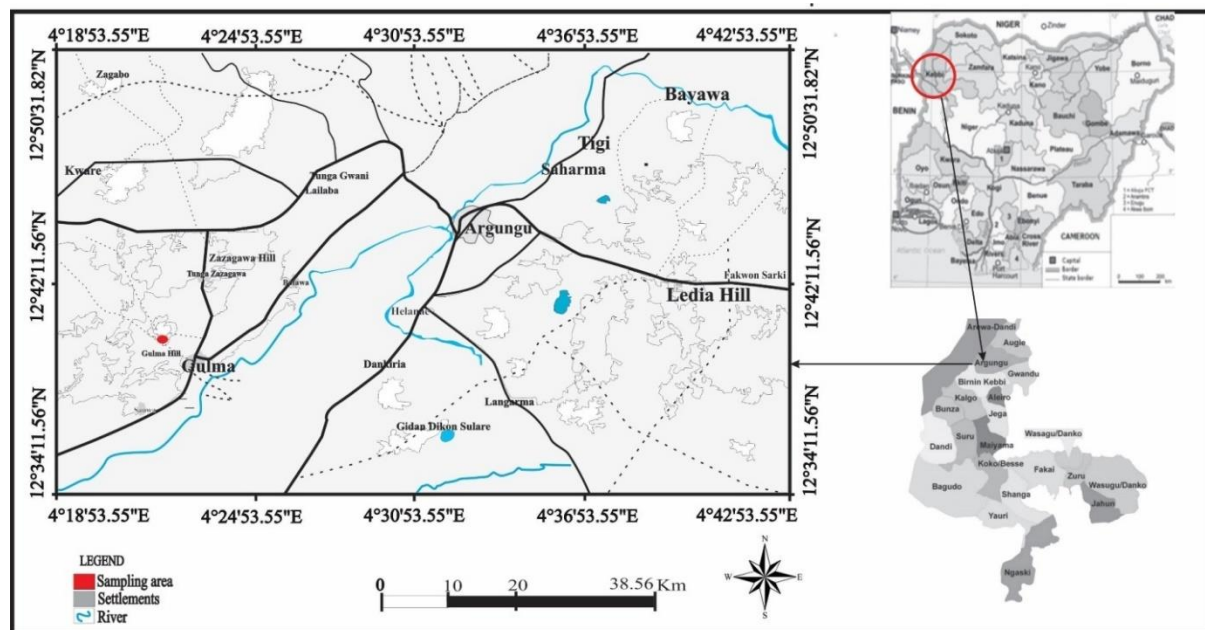


Fig. 1. Location map of the study area

2.0 Materials and Methods

Fieldwork was carried out with the aid of field materials such as a geological hammer, field note, pencil, marker pen, hand-lens, base map, compass, clinometer, GPS, measuring tape, masking tape, ruler, 10 % dilute hydrochloric acid and camera. Field study and logging of the bed succession was noted by taking cognizance of colour, rock type, mineral content, textural parameters, structure, fossil content, accessory minerals and diagenetic effect as detailed in the works of Ola-Buraimo (2020), Oladimeji and Ola-Buraimo (2022b), Ola-Buraimo and Usman (2022). Sieve analysis was carried out on dry disaggregated 100 g samples weighed by chemical balance. Set of sieves of various sizes, stacked, arranged from coarsest 2mm mesh at the top to 63 μ mesh with attached base pan. The set of sieves was tightly covered, fastened on the sieve shaker, and agitated for 15 minutes.

Thereafter, the grains retained in each sieve were weighed and recorded. These procedures were carried out for each of the six samples. Basic data, weighed or mass of the sediment each in a set of sieves were

input in Microsoft Excel format to generate a spreadsheet, graphical output (Blott, 2000). Statistics of the samples were calculated from the software, whereby, mean, sorting (standard deviation), skewness and kurtosis were derived in logarithmic using the phi scale of Krumbein and Pettijohn (1938). The software also utilized linear interpolation to calculate statistical parameters by Folk and Ward (1959) which gave resultant physical descriptions of textural attributes like moderately sorted, fine to medium grain sizes after Folk (1954). Grain size categorization into size fraction was generated, and modified after Udden (1914) and Wentworth (1922). Sample grain sizes were produced on triangular diagram to classify the sediments into sandstone classes (Blott, 2000).

Petrography preparation involved 100 g weight of sandstone, washed under running tap water in a 63 μ m mesh to remove clay particles present. After thorough washing, the sample was dried in an oven at high temperature. The sample was later mounted on a glass slide with Canada basal, and



ground to standard thickness before viewing under a petrographic microscope for mineralogical content and grain roundness. Heavy mineral preparation was by the use 10 g of the sample in duplicate. The sample was washed in 63 μm aperture to remove the clay particles. The washed sample was then boiled with hydrochloric acid (HCl) of 37 % purity for about ten minutes (10 min) in a fume cupboard. The boiled sample was then washed and dried the second time and ready for heavy mineral separation using the gravity method with bromoform ($\text{sg} = 2.8 \text{ g/cc}$) in a separating funnel. The extracted minerals were rinsed, dried, and mounted on a glass slide for heavy minerals study under a binocular microscope.

3.0 Results and Discussion

3.1 Lithological field description

Litho-description: The basal bed of the outcrop is composed of milky to purplish colour clay, slightly bioturbated with some burrows. The overlying bed is a yellowish nodular claystone, the nodules are in the pocket, and the claystone is also bioturbated. The nodules are distributed and aligned by striking NW-SE direction and they are dipping southward. The nodules have evidence of loadcast within the sharp contact and are associated with burrows.

The lower beds are overlain by milky to purple claystone; characterized by strongly bioturbated, thickly bedded and strongly fractured joints. The middle part of the outcrop shows a repetitive appearance of yellowish nodular claystone but fairly bioturbated, unlike the lower bed. The fairly bioturbated yellowish nodular claystone is overlain by reddish intercalated claystone. The contact between the yellowish nodular claystone and the intercalated reddish clay shows a wavy contorted contact. This may suggest a transition from a wavy marine environment to a continental environment, while the yellowish nodules impregnated within the clay facies decrease upward.

The reddish claystone of a possible continental environment is overlain by purple-coloured, thinly bedded, bioturbated

claystone, possibly of marine deposit. Towards the top of the outcrop is evidence of an upward shallowing from a relatively deep marine environment to a shallow marginal marine yellowish, highly bioturbated (Plt. 1), nodular claystone. The shallow marginal marine highly bioturbated, fossil cast (Plt. 2), nodular claystone has an undulating contact with the overlying thickly bedded, reddish mudstone. The topmost part of the outcrop is characterized by highly ferruginised granule stone of a fluviatile paleoenvironment of deposition. The Gulma Hill is unique in appearance with steep sites and a flat extensive top surface, associated with boulders and screes at the foot of the hill. A major fault was identified in the outcrop, having a structural relation with the adjoining hill. Therefore, the hill was defined as a footwall while the adjoining hill is a hanging wall (Plt. 3).

At location 2, the bed at the bottom is a kaolinitic claystone facies, strongly bioturbated and fractured, with a thickness of 5.8 m. This is overlain by structurally massive reddish claystone. The third layer is a thickly bedded sandstone, characterized by variegated whitish to purplish colour, a liesegang ring structure, bed that measures about 4.5 m in thickness. The liesegang ring structure is being reported here in Gwandu Formation for the first time (Plt. 4). The presence of the liesegang ring structure in the sandstone is posited as evidence of marine organic organisms' slime precipitation in the sandstone, deposited in the shallow marine environment (Oladimeji and Ola-Buraimo 2022). A similar liesegang ring structure was reported in Patti Sandstone, Patti Formation in Bida Basin along the Lokoja-Abuja Highway (Oladimeji and Ola-Buraimo, 2022). However, the liesegang ring structure present in the Gulma Sandstone Member Type Section is not lithified, but soft unlike the similar structure present in the Lokoja-Abuja Highway, known to be strongly lithified.





Plate 1. Bioturbation



Plate 2. Fossil cast



Plate 3. Fault zone: A. Hanging wall, B. Foot wall



Plate 4. Liesegang ring structure

Table 1. Summary of weight retained in sieve sizes for analyzed samples

| Sieve (mm) | Phi (Ø) | GR1 | GR2 | GR3 | GR4 | GR5 | GR6 |
|--------------|---------|-------|-------|-------|-------|-------|-------|
| 2.00 | -1.0 | 9.58 | 8.38 | 9.36 | 9.25 | 10.34 | 9.50 |
| 1.18 | -0.25 | 2.60 | 2.53 | 2.83 | 2.66 | 2.57 | 2.64 |
| 0.85 | 0.25 | 1.89 | 1.86 | 1.65 | 1.66 | 1.80 | 1.85 |
| 0.60 | 0.75 | 1.60 | 1.80 | 1.84 | 1.50 | 1.86 | 1.64 |
| 0.425 | 1.25 | 3.02 | 3.52 | 3.54 | 3.82 | 3.50 | 3.76 |
| 0.30 | 1.75 | 4.75 | 5.95 | 4.53 | 5.95 | 5.90 | 4.70 |
| 0.25 | 2.0 | 5.27 | 5.38 | 5.45 | 5.68 | 5.40 | 5.25 |
| 0.15 | 2.75 | 41.60 | 40.60 | 41.62 | 40.30 | 38.65 | 41.65 |
| 0.10 | 3.25 | 13.61 | 13.60 | 13.60 | 12.90 | 13.50 | 13.63 |
| 0.075 | 3.75 | 3.76 | 3.56 | 3.87 | 3.36 | 3.86 | 3.73 |
| 0.063 | 4.0 | 11.40 | 11.40 | 11.80 | 11.90 | 11.70 | 11.43 |
| Pan | 5.0 | 0.90 | 0.92 | 0.80 | 0.92 | 0.62 | 0.90 |
| Total | | 99.98 | 99.60 | 99.98 | 99.90 | 99.80 | 99.78 |

3.2 Sieve analysis result

The results obtained from the sieve analysis carried out on the six samples are presented in Table 1, while the cumulative weight obtained for each sample is presented in Tables 2 and 3. Table 1 indicates the respective weight retained in the sieve sizes.

The raw data obtained from the sieving exercises were plotted on a log graph for deducing textural parameters and statistical variables such as the mean, standard deviation (sorting), skewness and kurtosis. However, their interpretations were obtained from the cumulative frequency curve from



each sample as depicted in Figures 2a-7a and their respective histogram plots of their grain size distributions in Figures 2b-7b.

Thereafter, the statistical data obtained from the grain size parameters and their respective interpretations were presented in Table 4. Samples 1-6 have various means, standard

deviation (sorting), skewness and kurtosis values as shown in Table 4. The mean values for the six sandstone samples range from 2.2 to 2.26 with an average value of 1.86. This was interpreted that the Gulma Sandstone belongs to a fine sandstone classification (Table 4).

Table 2 Summary of the cumulative weight of analyzed samples

| Phi (Ø) | Wt. of Sample GR1 | Wt. of Sample GR 2 | Wt. of Sample GR 3 | Wt. of Sample GR 4 | Wt. of Sample GR 5 | Wt. of Sample GR 6 |
|---------|-------------------|--------------------|--------------------|--------------------|--------------------|--------------------|
| -1.0 | 9.8 | 8.38 | 9.36 | 9.25 | 10.34 | 9.50 |
| -0.25 | 12.18 | 10.91 | 11.89 | 11.91 | 12.91 | 12.14 |
| 0.25 | 14.07 | 12.77 | 13.54 | 13.57 | 14.71 | 13.99 |
| 0.75 | 15.67 | 14.57 | 15.38 | 15.07 | 16.57 | 15.63 |
| 1.25 | 18.69 | 18.09 | 18.92 | 18.89 | 20.07 | 19.39 |
| 1.75 | 23.44 | 24.04 | 23.45 | 24.84 | 25.97 | 24.09 |
| 2.0 | 28.71 | 29.42 | 28.90 | 30.68 | 31.37 | 29.34 |
| 2.75 | 70.31 | 70.02 | 70.52 | 70.82 | 70.02 | 70.99 |
| 3.25 | 83.92 | 83.62 | 84.12 | 83.72 | 83.52 | 84.62 |
| 3.75 | 87.68 | 87.18 | 87.99 | 87.08 | 87.38 | 88.35 |
| 4.0 | 99.08 | 98.58 | 99.99 | 98.78 | 99.08 | 99.78 |
| 5.0 | 99.98 | 99.50 | 100.59 | 99.70 | 99.70 | 100.68 |

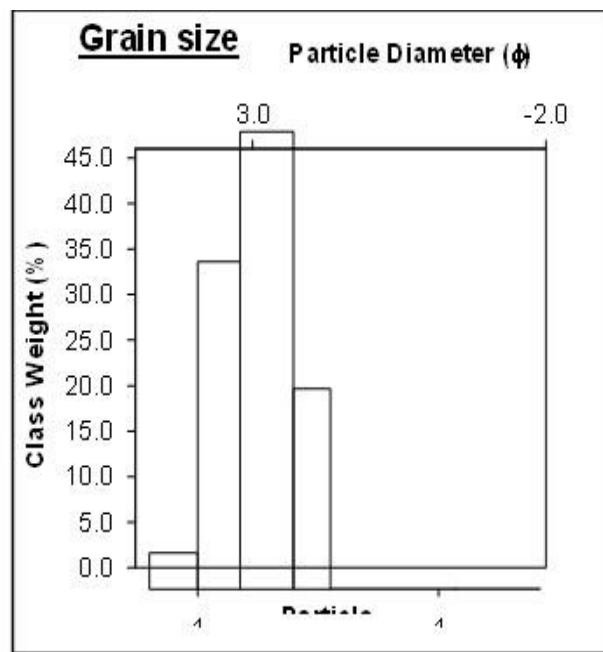
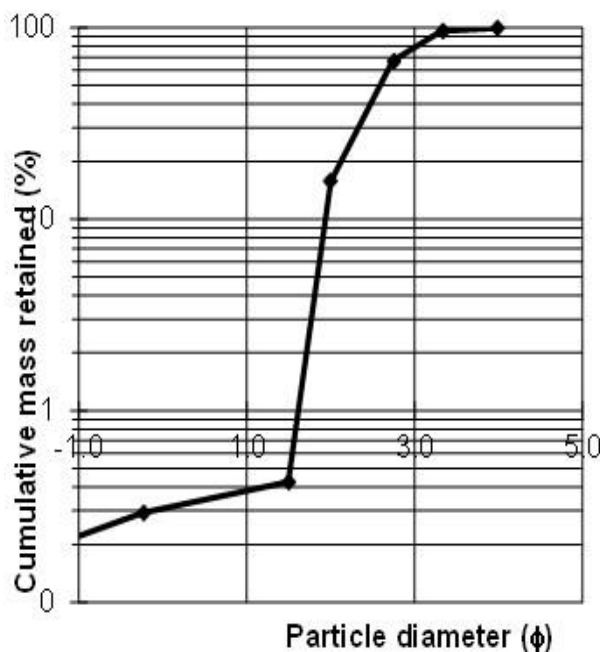


Fig. 2a; Cumulative curve for Sample GR1

Fig. 2b: Grain size distribution in Sample GR1



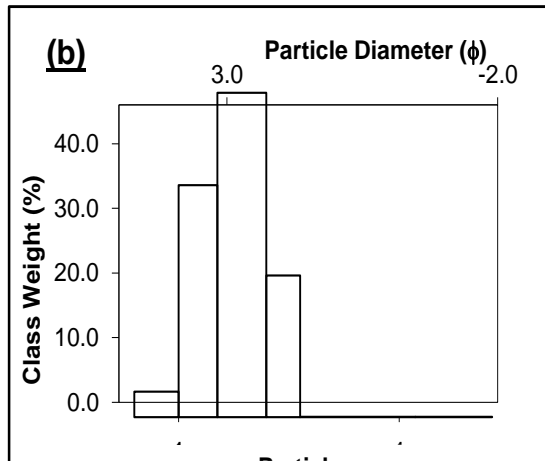
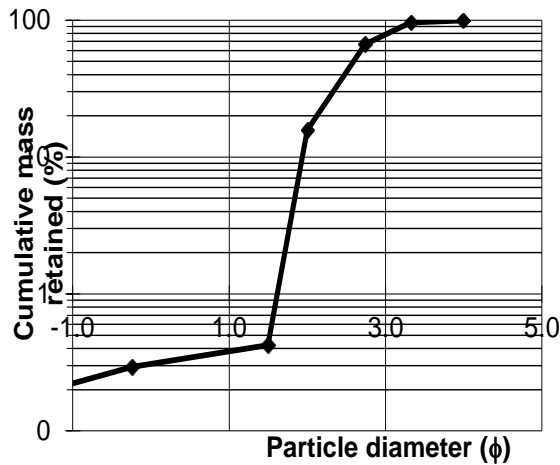


Fig. 3a: Cumulative curve for Sample GR2 Fig. 4.3b: Grain size distribution in Sample GR2

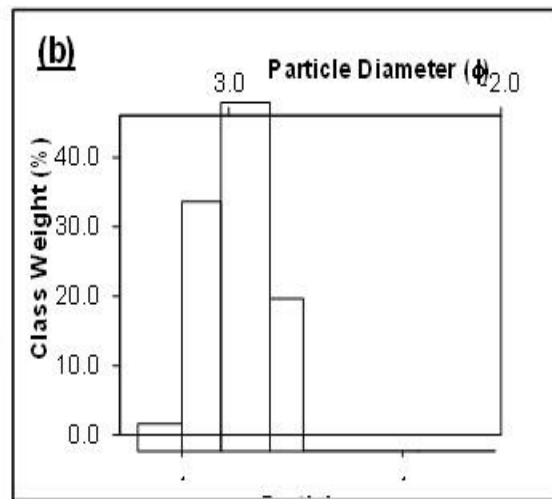
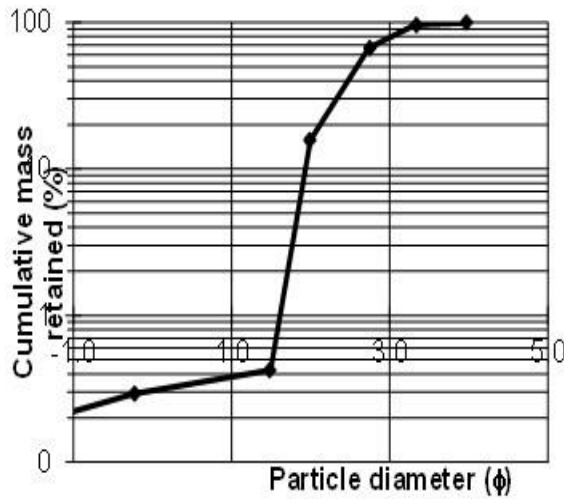


Fig. 4a: Cumulative curve for Sample GR3 Figure 4b: Grain size distribution in Sample GR3

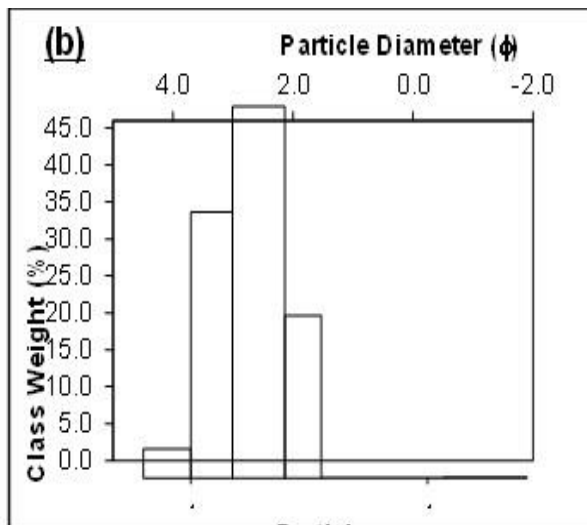
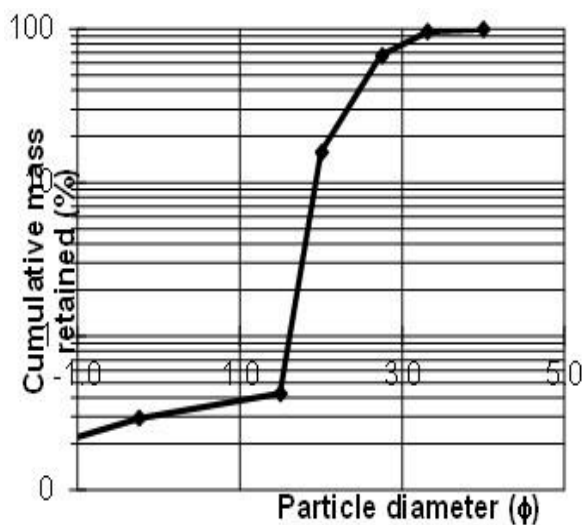


Fig. 5a: Cumulative curve for Sample GR4 Fig. 5b: Grain size distribution in Sample GR4



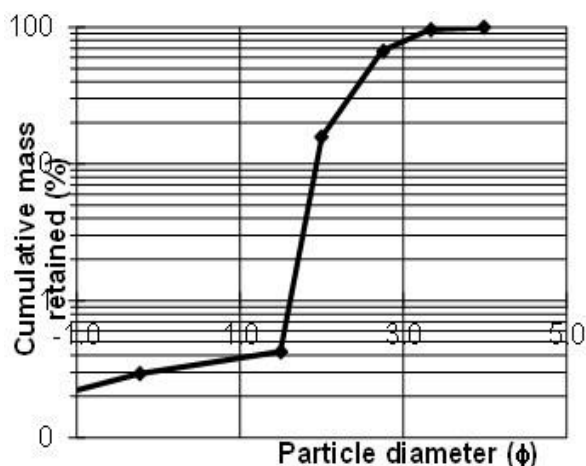


Fig. 6a: Cumulative curve for Sample GR5

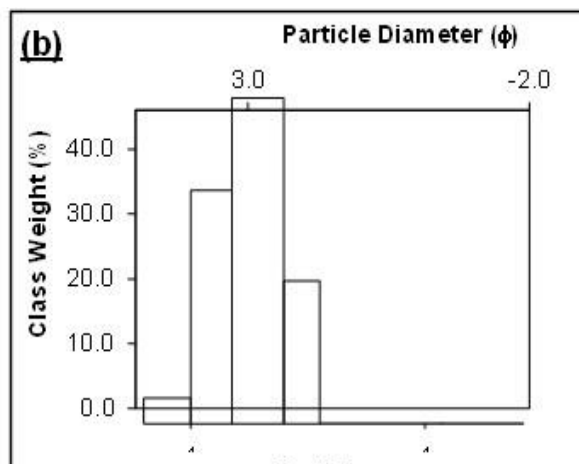


Fig. 6b: Grain size distribution in Sample GR5

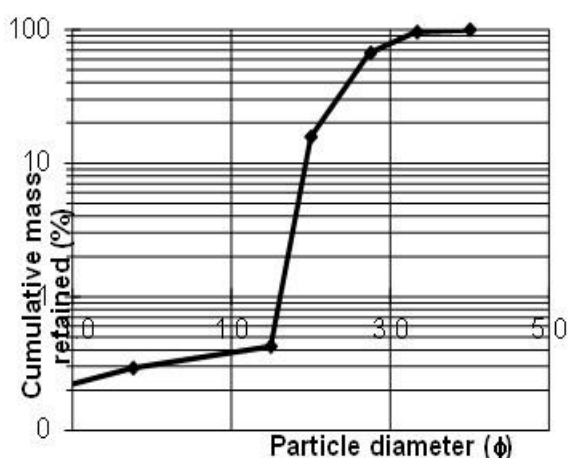


Fig 7a: Cumulative curve for Sample GR6

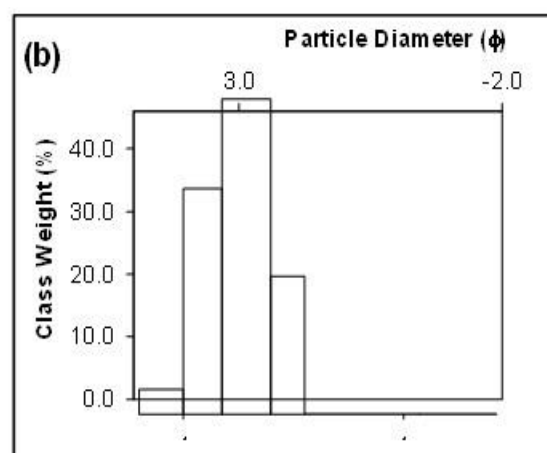


Fig. 7b: Grain size distribution in Sample GR6

The particle sizes for the Gulma Sandstone samples suggest that the sediments were transported far away from the source for them to achieve fine sand-size deposits. The sorting behaviours are demonstrated by the samples having sorting values ranging from 1.2-1.216 with an average value of 1.196, suggestive of poorly sorted sediment class. The poorly sorted nature of the Gulma Sandstone suggests transportation that was in phases, characterized by multiple channels of transportation with fluctuated energy current of transportation. The late stage of the sediments transport mechanism was low energy of transportation, possibly interjected by turbulent phases, deposited by high sedimentation rate, and resulted in poorly sorted particles (Tab. 4). The sediments of samples 1-6 are terrigenous, possibly transported from the continent by turbidity

current, deposited partly in intertidal and tidal shelf setting characterized by the intermittent supply of marine water, thereby, allowed the precipitation of slime produced by marine organisms to form liesegang structure within the deposited sediment in a marginal marine environment.

Skewness values from Table 4 show that the values vary between -0.447 to -0.1. The skewness values were classified into coarse skewed. The coarse skewed class is defined by particle assemblage having a coarse-grained size at its tail. This implies a dominant fine-grained sediment characterized by the presence of some relatively coarse particles which were present at the tail of the skewness (Figs. 2a-7a). This resulted from the effect of the intermittent tidal current effect, a dominant factor responsible for the deposition of the Gulma



Sandstone. This phenomenon is similar to the tidal deposit of sediment in Dukku Sandstone (Ola-Buraimo *et al.*, 2022).

Kurtosis is a measure of how peak a symmetry is in terms of grain size distribution (Ola-Buraimo *et al.*, 2022). Three classes of kurtosis were interpreted from the data and presented in Table 4. The kurtosis values range from 0.7-1.82 with an average value of 1.335. The classes of kurtosis established are very leptokurtic, platykurtic and leptokurtic. The leptokurtic class of samples are Samples 4 and 6, described to exhibit unimodal sources of sediments. The leptokurtic is more peaked than the normal curve. The second type of kurtosis is very leptokurtic with Samples 1 and 2, also of unimodal source.

The platykurtic class of kurtosis indicates that the sediments from Samples 3 and 5 are polymodal in terms of sources of the sediments, otherwise referred to as multiple sources (Tab. 4). This factor might be responsible for the reason why the sediments are poorly sorted in nature due to multiple supply of sediments, characterized by various regimes of transportation and depositional conditions.

The gravel-sand-mud ternary diagram plot in Figure 8 shows that the Gulma sediment is of sandstone particles. A similar plot of sand-silt-clay ternary diagram (Fig. 9) also indicates that the Gulma particles are majorly sand-size grains.

Table 4. Summary of statistical grain size parameters and their interpretation

| Sample name/Statistical Parameters | GR 1 | GR 2 | GR 3 | GR 4 | GR 5 | GR 6 |
|--|-------------------------------|-------------------------------|----------------------|-------------------------------|-------------------------------|-------------------------------|
| Mean value (π) | 2.26 | 2.23 | 2.23 | 2.2 | 2.2 | 2.23 |
| Mean description | Fine sand | Fine sand | Fine sand | Fine Sand | Fine Sand | Fine Sand |
| Sorting value (σ) | 1.23 | 1.20 | 1.156 | 1.216 | 1.175 | 1.2 |
| Sorting description | Poorly Sorted | Poorly Sorted | Poorly Sorted | Poorly Sorted | Poorly Sorted | Poorly Sorted |
| Skewness value (SK) | -0.1 | -0.132 | -0.447 | -0.15 | -0.154 | -0.21 |
| Skewness description | Coarsely or Negatively Skewed | Coarsely or Negatively Skewed | Very Coarsely skewed | Coarsely or Negatively Skewed | Coarsely or Negatively Skewed | Coarsely or Negatively Skewed |
| Kurtosis value (K) | 1.82 | 1.6 | 0.7 | 1.45 | 0.94 | 1.5 |
| Kurtosis description | Very Leptokurtic | Very Leptokurtic | Platykurtic | Leptokurtic | Platykurtic | Leptokurtic |

3.3 Paleoenvironment of deposition

The paleoenvironment of deposition of Guluma Sandstone was deduced by calculating multivariate values for the

sediments of samples 1-6 following Sahu (1964) using a formula:

$$MV = 0.2852Mz - 8.76045 - 4.8932SKI + 0.0482KG$$

where Mz = Grain size value, SKI = Skewness value, KG = Kurtosis value



The results obtained from the calculation of the multivariate values for the analyzed samples are presented in Table 5 below. The multivariate values of Gulma Sandstone

samples are depictive of tidal to intertidal environment of deposition.

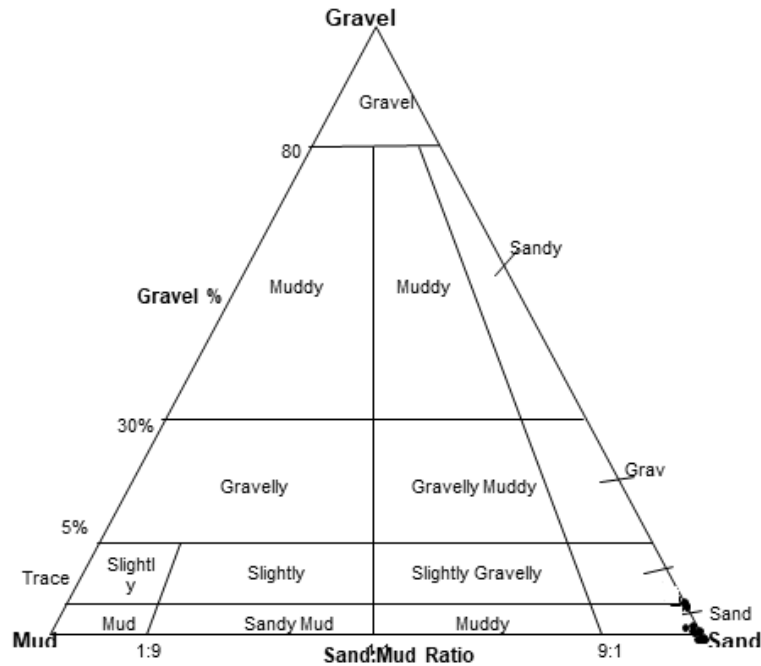


Fig. 8. Gravel-Sand-Mud ternary diagram of Gulma Sandstone

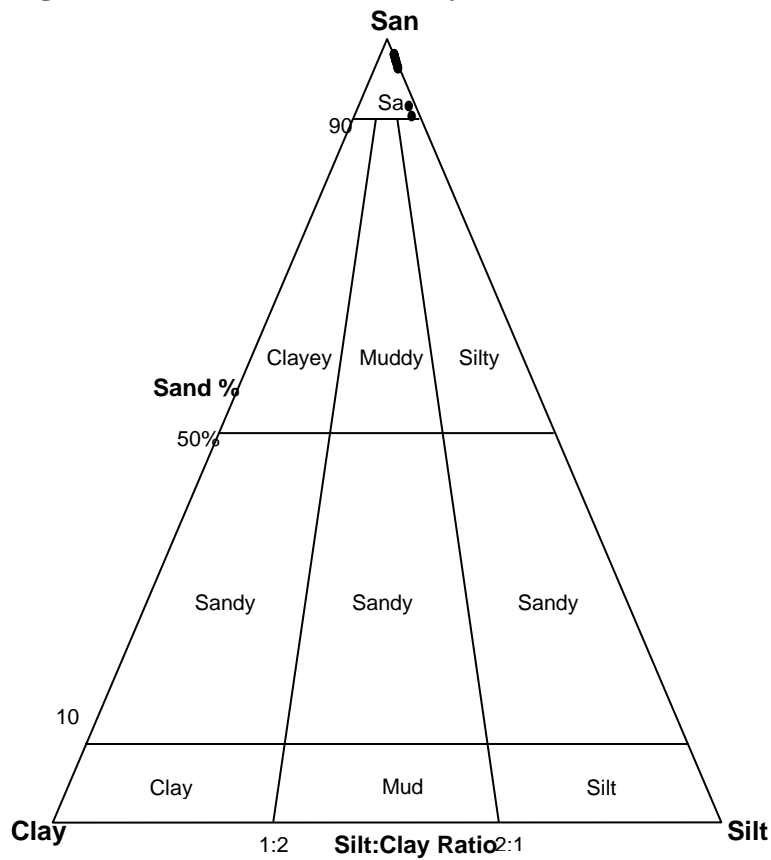


Fig. 9. Sand-Silt-Clay ternary diagram of Gulma Sandstone



Table 5: Multivariate values for paleoenvironment of deposition (after Sahu, 1964)

| Sample name | Grain size (Mz) | Skewness (SKI) | Kurtosis (KG) | Multivariate value (MV) | Depositional Setting | Depositional System |
|-------------|-----------------|----------------|---------------|-------------------------|----------------------|---------------------|
| GR 1 | 2.26 | -0.1 | 1.82 | -7.54 | Intertidal | Marginal marine |
| GR 2 | 2.23 | -0.132 | 1.6 | -7.40 | Intertidal | |
| GR 3 | 2.22 | -0.447 | 0.7 | -5.90 | Tidal shelf | |
| GR 4 | 2.22 | -0.15 | 1.45 | -7.32 | Intertidal | |
| GR 5 | 2.23 | -0.154 | 0.94 | -7.33 | Intertidal | |
| GR 6 | 2.23 | -0.21 | 1.5 | -9.07 | Intertidal | |

3.4 Heavy mineral

The results obtained from the heavy minerals analysis of the Gulma Sandstone under the microscope and their respective quantity abundance are given in Table 6.

Table 6: Heavy mineral separation count

| Sample No. | Zircon (Z) | Tourmaline (T) | Rutile (R) | Epidote (Ep) | Apatite (Ap) | Garnet (G) | Staurolite (St) | Opaque (Op) | ZTR Index |
|----------------|------------|----------------|------------|--------------|--------------|------------|-----------------|-------------|-----------|
| GR 1 | 28 | 15 | 19 | 6 | 5 | 7 | 22 | 80 | 77.5 |
| GR 2 | 22 | 13 | 24 | 5 | 8 | 4 | 18 | 89 | 73.75 |
| GR 3 | 18 | 15 | 22 | 4 | 3 | 5 | 14 | 75 | 68.75 |
| GR 4 | 22 | 17 | 20 | 4 | 4 | 3 | 16 | 79 | 73.75 |
| GR 5 | 19 | 12 | 15 | 3 | 2 | 8 | 16 | 55 | 57.5 |
| GR 6 | 18 | 10 | 12 | 4 | 3 | 7 | 12 | 74 | 53.75 |
| Average | 21.2 | 13.67 | 18.67 | 4.33 | 4.16 | 5.66 | 16.33 | 75.33 | 55.22 |

Heavy mineral assemblage suits of the samples containing Zircon, Rutile, Tourmaline, Epidote, Apatite, Garnet, Staurolite and other opaque minerals show no particular trend in their point count. However, zircon has the highest mineral count between 18-28 (ave. 21.2). It is a non-silicate mineral which occurs as an accessory constituent of felsic igneous rocks such as granite and metamorphic facies such as gneiss and detrital deposits (Gujar and Rajmanickam, 2007). Rutile ranked second in the abundance of the mineral suit recovered from the sediment samples. It ranges in abundant count from 12-24, with an average count of 18.67. It occurs commonly as an accessory mineral in igneous rock and many granite, diorite and metamorphic derivatives such as gneisses, and amphibolite; including other grades of metamorphism such as mica schist and high grade metamorphism.

Tourmaline ranked third most abundant mineral. It ranges from 10-17 (ave. 13.67). It usually formed during hydrothermal activity of metamorphic rocks; occurs in granitic pegmatite, schist and commonly in detrital materials. The occurrence of Zircon, Rutile and Tourmaline in the sediments indicates an acid igneous rock and metamorphic (bimodal) sources (Feo-codecido, 1956; Ola-Buraimo and Usman 2022, Ola-Buraimo *et al.*, 2022). This substantiates the fact that the Gulma Sandstone deposit was a multi-sourced sediment, and another major factor responsible for the poor sorting nature of the sandstone.

However, mineralogy maturity was determined by adopting the composition maturity index calculated after the work of Hubert (1962). This was based on the point count of Zircon, Tourmaline, Rutile and



non-opaque heavy minerals; computed for each sample using the formula:

$$ZTR = \frac{Zircon+Tourmaline+Rutile \times 100}{Number\ of\ non\ opaque} \quad (1)$$

The calculated percentages of the determinant heavy minerals such as the zircon, tourmaline and rutile were recorded in Table 6. The ZTR Index for the samples are moderately high, ranging from 53.75-77.5 with an average value of 67.5. A relatively high ZTR Index percentage recorded for the samples suggests sub-matured to mature sediments that had been transported far away from the parent source rocks, but being affected by intermittent discharge of coarse materials, deposited by tidal current in a marginal marine environment.

ZTR Index < 50 % was classified as immature (Hubert, 1964), ZTR > 50 %, but < 76 % was classified as sub-mature (Ola-Buraimo *et al.*, 2022), while ZTR Index greater > 76 % was considered to be matured sediments. Therefore, Sample

GR1 with ZTR Index of 77 % (> 76 %) was classified as the only mineralogically mature sediment. All other samples with ZTR Index > 50 % but < 76 % were classified as mineralogically sub-mature sediments. Generally, the Guluma Sandstone can be described to be a mineralogically sub-mature sandstone. Figure 10 shows a graphical expression in bar chart of ZTR Index for Samples 1-6. The sediments of Samples 1- 6 are suggested to be transported by turbidity current, whereby, the sediments were carried from the continental environment under low energy of transportation, deposited in the marine environment, but subjected to the effect of tidal influence whereby coarse materials were intermittently mixed with dominant fine-grained particles during the high tide. Therefore, the transportation and deposition processes did not give enough room for the sediments to achieve mineralogical maturity.

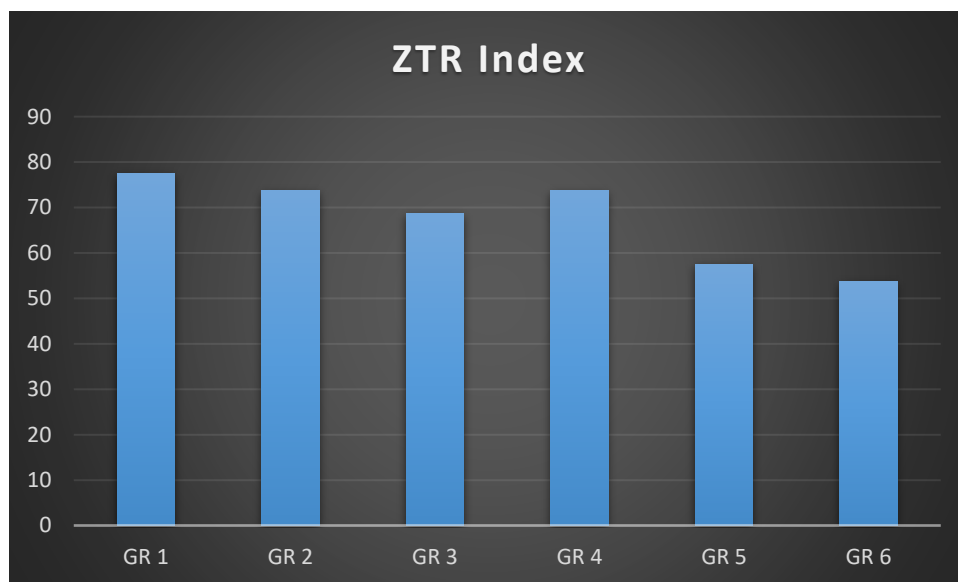


Fig. 10: Graphical representation of ZTR Index for Guluma Sandstone

3.5 Mineralogical Maturity Index

The mineralogical maturity index (MMI) of the Guluma Sandstone samples is contained in Table 7. This was obtained by petrographic point count of quartz, feldspar, and rock fragments. MMI was calculated using the

parameters in Table 7 as proposed by Nwajide and Hoque (1985). The mineralogical maturity index was determined using the expression:

$$MMI = \frac{Proportion\ of\ quartz}{Proportion\ of\ fsp - proportion\ of\ RF} \quad (2)$$



The MMI values range between 1.11 and 2.35 with an average value of 1.61. This suggested that the sediments are mineralogically immature (Table 7). The results obtained are classified in the Q= 75-50 % (F+RF) = 25-50 % with MMI equivalent of 3.0-1.0, interpreted to be mineralogically immature (Nwajide and

Hoque,1985). The petrographic microphotographs show the roundness of the sediments to vary from sub-angular to rounded, suggestive of a texturally sub-mature sediment, subjected to multiple directional currents in a marginal marine environment (Plate 5).

Table 7. Composition of sandstone facies studied and the mineralogical maturity index

| SAMPLE ID | Quartz (Qtz) | Feldspar (Fsp) | Rock (lithic fragment)(RF) | Fsp+Rf | % Qtz | % Fsp+Rf | Mineralogical maturity index (MMI) |
|-----------|--------------|----------------|----------------------------|--------|-------|----------|------------------------------------|
| GR1 | 67 | 24 | 36 | 60 | 72.3 | 63.3 | 1.11 |
| GR2 | 75 | 34 | 28 | 62 | 78 | 65.4 | 1.20 |
| GR3 | 83 | 41 | 18 | 59 | 86.5 | 64.3 | 1.40 |
| GR4 | 88 | 37 | 15 | 52 | 91.2 | 55.8 | 1.69 |
| GR5 | 83 | 25 | 19 | 44 | 88.5 | 46.4 | 1.89 |
| GR6 | 92 | 25 | 14 | 39 | 95.2 | 43.6 | 2.35 |
| AVERAGE | 81.33 | 31.0 | 21.67 | 52.66 | 85.29 | 56.47 | 1.61 |

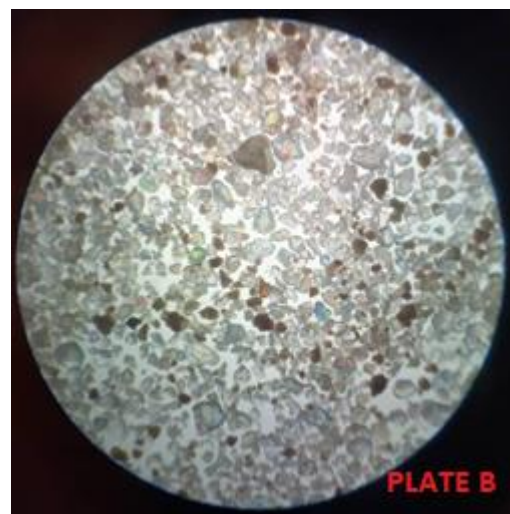
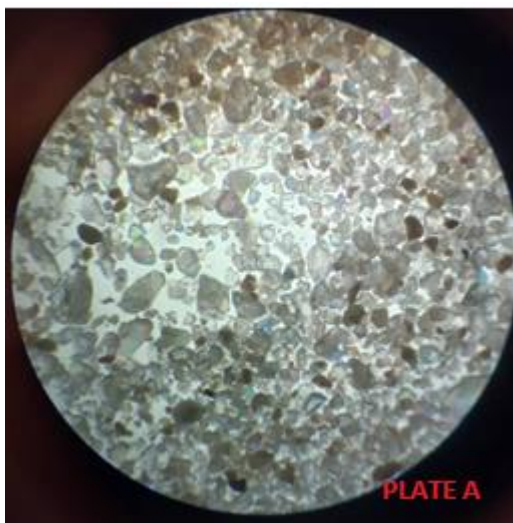


Plate 5 (A and B). Point count of Quartz, Feldspar, and Rock Fragments and grain roundness

4.0 Conclusion

The outcrop litho-section of the Gulma Hill is composed of nine repetitive beds. The lithofacies are purple-coloured liesegang ring structure sandstone, moderately bioturbated claystone, yellowish nodular claystone, and continental massive reddish claystone. The

topmost beds are continental massive reddish mudstone and ferruginized granule-stone as the capping rock, which is characteristically different from the commonly described oolitic ironstone that characterized the top of the Gwandu Formation. Liesegang ring structure is characteristically present and reported for the first time in Gwandu Formation.



Textural statistical parameters derived in the mean, standard deviation (sorting), skewness and kurtosis show that the mean values of the samples have an average of 1.86, suggestive of fine sand facies. The sorting average value is 1.196, indicative of poorly sorted sediment, deposited by the tidal current of high energy. The skewness is negatively skewed, Kurtosis vary from very leptokurtic, through platykurtic to leptokurtic classes. The paleoenvironment of deposition deduction vary from -9.07 to -5.90; suggestive of marginal marine setting of an intertidal and tidal shelf deposit. The Gulma Sandstone is texturally submatured because the grains are sub-angular to rounded in angularity, and mineralogically submature.

5.0 Acknowledgement

The authors thank the field teammates for the cooperation and assistance rendered in the field during the gathering of geologic information. We appreciate the cooperation and assistance of Mr. Abdulwaheed, the laboratory technologist, and the Department of Geology, Federal University Birnin Kebbi for permitting us to use the Sedimentology Laboratory. Our gratitude is also extended to Palystat Limited for the provision of literatures used for this research. We sincerely thank the contribution of the unanimous reviewer for improving the quality of the paper.

5.0 References

- Blott, S. (2000). A grain size distribution and statistic package for the analysis of unconsolidated sediments by sieving or laser granulometer. *Department of geology, Royal Holloway, University of London*.
- Falconer, J.D. (1911). The geology and geography of Northern Nigeria. *Macmillan London*, 295p.
- Feo-codecido, G. (1956). Heavy Mineral techniques and their Application to Venezuelan Stratigraphy. *Bulletin of the American Association of Petroleum Geologists*, 5: 984-1000.
- Folk, R.L. (1954). The distinction between grain size and mineral composition in sedimentary-rock nomenclature. *Journal of Geology*, 62, 344-359.
- Folk, R.L. and Ward, W.C. (1957). Brazos River bar: a study in the significance of grain size parameters. *Journal of Sedimentary Petrology*, 27: 3-26.
- Gujar, A.R. and Rajamanickam, G.V. (2007). Characterization and application of naturally occurring mineral-based pigment in surface coating. *Journal of Minerals and Materials Characterization and Engineering*, 6(1): 53-67.
- Hamidu, I., Umar, Z.F., Ibrahim, H. A., Halidu, H. and Haruna, G.M. (2024). High-resolution sequence stratigraphy of the Maastrichtian-Paleocene succession in the Sokoto Basin. *Arabian Journal of Geosciences*, 17(54): 1-13.
- Hubert, J.F. (1962). A Zircon-Tourmaline-Rutile maturity index and the interdependence of the composition of heavy mineral assemblages with the gross composition and texture of sandstones. *Journal of sedimentary petrology*, 32(3): 440-450.
- Kogbe C.A. (1979). Geology of the south-eastern (Sokoto) sector of the Lullemeden Basin. *Dept. of Geology Ahmadu Bello University, Zaria Bulletin*, 1-142.
- Kogbe, C.A. (1981). Cretaceous and Tertiary of the Iullemmenden Basin of Nigeria (West Africa). *Creac. Res.* 2: 129-186.
- Kogbe, C.A. (1989). The Cretaceous and Paleogene sediments of southern Nigeria. In: Kogbe, C. A., Ed., *Geology of Nigeria. Elizabethan publishers, company, Lagos*, 325-334.
- Krumbein, W.C. and Pettijohn, F.J. (1938). *Manual of Sedimentary Petrography*. Appleton-Century-Crofts, New York.4



- Nwajide, C.S. (2013). Geology of Nigeria's sedimentary basins. *CSS Bookshop Limited*.
- Obaje, N.G. (2009). Geology and mineral resources of Nigeria. *Springer, Heidelberg*, 221p.
- Obaje, N.G., Adukub, M. and Yusuf, I. (2013). The Sokoto Basin of Northwestern Nigeria: a preliminary assessment of the hydrocarbon prospectivity. *Pet. Technol. Dev. J.* 3(2): 66-80.
- Obiosio, E.O., Obaje, N.G. and Okosun, E.A. (1998). Foraminiferal paleoecology of the Kalabaina Limestone, southeastern sector of the Iullemeden Basin, Sokoto, Nigeria. *Journal of Mining and Geology*, 34: 19-25.
- Ola-Buraimo, A.O. (2020). Palynozonation and chronostratigraphy of the Albian to Pliocene sediments of the Nzam-1, Umuna-1 and Akukwa-2 Wells Anambra Basin, southeastern Nigeria. *University of Ibadan, PhD thesis*, 182p.
- Ola-Buraimo, A.O. and Haidara, N. (2022). Pollen and Spores Recovery in Tunga Buzu Carbonaceous Shale Type Section Member: Significance in sequence stratigraphy, age dating and paleoenvironment deduction of the Early Miocene Gwandu Formation, Sokoto Basin, Northwestern Nigeria. *British Journal of Earth Sciences Research*, 10(3): 16-25.
- Ola-Buraimo, A.O. and Meshack, B.H. (2024). Foraminifera and sequence stratigraphy study of the Early Maastrichtian to Paleocene sediments of Kalambaina Formation, Sokoto Basin, northwestern Nigeria (in press).
- Ola-Buraimo, A.O. and Mohammed A.T. (2024). Palynological zonation and age dating of the Gamba (Middle Eocene) and Kalambaina (Early Maastrichtian-Paleocene) Formations, Sokoto Basin, northwestern Nigeria (in press).
- Ola-Buraimo, A.O., Oladimeji, R.G. and Abdulmutalib, S. (2023). Textural and Depositional Paradigm of Middle Neritic Environmental System of Kola Siltstone Type Section, Gwandu Formation, Sokoto Basin, Northwestern Nigeria. *Minna Journal of Geosciences*, 6(1&2): 76-92.
- Ola-Buraimo, A.O., Oladimeji, R.G. and Badamosi, B. (2023). Geochemical and Petrographic Studies: Implication on the Mineralogical Maturity, Sedimentation Processes and Paleoenvironment of Deposition of Jodu Sandstone, Gwandu Formation, Sokoto Basin, Northwestern Nigeria. *International Journal of Innovative Environmental Studies Research*, 11(1): 1-11.
- Ola-Buraimo, A.O., Ologe, O. and Benemaikwu, O.D. (2018). Field geology and microbiological investigation of borehole, public tap water and hand-dug wells in some parts of Birnin Kebbi, Nigeria. *Nigerian Journal of Scientific Research*, 17(3): 322-333.
- Ola-Buraimo, A.O., Oladimeji, R.G. and Faruk, A.K. (2022). Palynology, paleoenvironment and stratigraphy relationship of Tungan Buzu Hill with adjacent valley Gwandu Formation, Sokoto Basin, Northwestern Nigeria. *African Journal of Environment and Natural Science Research*, 5(2): 15-26.
- Ola-Buraimo, A.O., Oladimeji, R.G. and Imran, M. (2022). Sandstone textural properties and paleoenvironment of Deposition of Dukku Sandstone Type Locality, Gwandu Formation, Sokoto Basin, Northwestern Nigeria. *International Journal of Innovative Environmental Studies Research* 10(3): 39-55.
- Ola-Buraimo, A.O. and Usman S.K.H. (2022). Geochemistry, textural and mineralogical maturity indices of Dukku Sandstone Member, Type Section of Gwandu Formation, Sokoto Basin, Northwestern Nigeria. *Savanna Journal of Basic and Applied Sciences*, 4(2): 1-16.



- Oladimeji, R.G. and Ola-Buraimo, A.O. (2022). Textural and paleoenvironmental characterization of the Campano-Maastrichtian Patti Sandstone, Southern Bida Basin, Northcentral Nigeria. *Petroleum and Petroleum Engineering Journal*, 6(2): 1-11.
- Ozumba, M.B., Chima, K.I., Nwajide, C.S., Farouk, U.Z., Umar, A.R. (2017). Attributes of potential hydrocarbon reservoir sandstones in the Sokoto Sector of the Iullemmenden Basin: An outcrop analogue study. *Archives of Petroleum Environmental Biotechnology*. 2017(4): 1-9.
- Sahu, R. (1964). Textural parameters: An evaluation of fluvial and shallow marine deposits. *Journal Sedimentary Petrology*, 34: 513-520.
- Udden, J.A. (1914). Mechanical composition of clastic sediments. *Bulletin of the Geological Society of America*, 25: 655-744.
- Wentworth, C.K. (1922). A scale of grade and class terms for clastic sediments. *Journal of Geology*, 30: 377-392.

**Compliance with Ethical Standards
Declarations**

The authors declare that they have no conflict of interest.

Data availability

All data used in this study will be readily available to the public.

Consent for publication

Not Applicable

Availability of data and materials

The publisher has the right to make the data Public.

Competing interests

The authors declared no conflict of interest.

Funding

There is no source of external funding

Authors' contributions

The first author contributed 70 %, second author contributed 30 %

